

# Novel PRF Schedules for Medium PRF Radar

Evan J. Hughes\*, Clive M. Alabaster†  
Department of Aerospace, Power and Sensors,  
Cranfield University,  
Royal Military College of Science,  
Shrivenham, Swindon,  
England, SN6 8LA.  
\*ejhughes@iee.org  
†C.M.Alabaster@rmcs.cranfield.ac.uk

**Abstract**— Previous work has demonstrated that Evolutionary Algorithms (EAs) are an effective tool for the selection of optimal pulse repetition frequency (PRF) sets to minimise range-Doppler blindness of a medium PRF radar. This paper re-considers the concepts of decodability in medium PRF radar, and how new and novel schedules can be generated using an EA. Traditionally target data is required in a minimum of 3 PRFs (e.g. a 3 of 8 scheme). In this paper we describe the generation of schedules requiring data in only 2 PRFs. Results are presented for a comparison between schemes requiring target data in two and three PRFs. The results indicate that blindness is minimised in schedules with greater numbers of PRFs and requiring target data in fewer PRFs. The concept of dynamic selection of PRI schedules that are fully decodable and have no blind velocities is outlined and is concluded to be feasible.

## I. INTRODUCTION

Many modern radar systems use medium pulse repetition frequency (PRF) waveforms to measure both target range and velocity accurately and unambiguously in the presence of clutter. Medium PRF radars possess excellent clutter rejection characteristics which render them an attractive proposition for airborne intercept (AI), fire control systems, ground based air surveillance, weapon locating radar and a variety of other applications.

A radar using a single medium PRF generates highly ambiguous range and Doppler data and suffers from a number of blind regions in range and velocity. The ambiguities may be resolved by operating on  $N$  PRFs, typically eight, and requiring target data in a minimum number,  $M$ , typically three, in what is known as a generally known as an  $M$  of  $N$  (3 of 8) scheme. The problem becomes one of selecting suitable combinations of PRFs to resolve the ambiguities, minimise the blind zones, avoid blind velocities and reduce problems of ghosting, whereby incomplete resolution of the ambiguities in the presence of noise can lead to false targets.

The spread of PRFs is governed by sound engineering principles, based on clutter rejection and target illumination times. However, the traditional approach to the selection of precise values often results in mediocre radar performance. Previous work by the authors [1], [2] has shown that it is possible to use evolutionary algorithms to automate the process of generating near-optimal PRF sets that minimise the blind zones for a detailed radar model. The previous work focussed

on generating both 3 of 8 and 3 of 9 schedules which are common in airborne intercept radars. This paper takes a fresh look at the problems of ambiguity resolution in medium PRF radar and proposes a new and very novel scheme that requires only two PRFs for target detection.

Section II describes the factors influencing the choice of PRF sets for a medium PRF radar and of the proposed timing rationale. Section III details the concept of decodability and introduces 2 of  $N$  schedules. Section IV presents a radar model based on an airborne fire control type radar. Section V describes the evolutionary algorithm and how it is applied to the problem. Section VI discusses issues involved with optimising the PRF set dynamically and section VII compares the performance of 2 of  $N$  systems with the more traditional 3 of  $N$ . This paper concludes that a 2 of 6 system has better blind zone performance than a 3 of 8 system and by using the evolutionary approach, solutions can be found that are fully decodable and avoid blind velocities. The option of reconfiguring the PRF set dynamically with changes in platform motion and clutter backscatter is now possible.

## II. MEDIUM PRF RADAR

### A. Introduction

Medium-PRF radar is a compromise solution designed to overcome some of the limitations of both low and high-PRF radar [3]. By operating above the low-PRF region, the ambiguous repetitions of the mainbeam clutter spectrum may be sufficiently separated without incurring unreasonable range ambiguities. Consequently, the radar is better able to reject mainbeam clutter through Doppler filtering without rejecting too many targets. By operating below the high-PRF region, the radar's ability to contend with sidelobe clutter in tail-chase engagements is improved. Targets may be extracted from sidelobe clutter using a combination of Doppler filtering and range gating.

### B. PRF Selection

Each PRF is characterised by regions of blind velocities and ranges associated with the Doppler filtering of mainbeam clutter and time gating of sidelobe clutter and associated eclipsing losses. These blind zones are depicted in black on a blind zone map (see Fig. 1).

## Report Documentation Page

*Form Approved*  
*OMB No. 0704-0188*

Public reporting burden for the collection of information is estimated to average 1 hour per response, including the time for reviewing instructions, searching existing data sources, gathering and maintaining the data needed, and completing and reviewing the collection of information. Send comments regarding this burden estimate or any other aspect of this collection of information, including suggestions for reducing this burden, to Washington Headquarters Services, Directorate for Information Operations and Reports, 1215 Jefferson Davis Highway, Suite 1204, Arlington VA 22202-4302. Respondents should be aware that notwithstanding any other provision of law, no person shall be subject to a penalty for failing to comply with a collection of information if it does not display a currently valid OMB control number.

1. REPORT DATE <b>14 APR 2005</b>	2. REPORT TYPE <b>N/A</b>	3. DATES COVERED <b>-</b>			
4. TITLE AND SUBTITLE <b>Novel PRF Schedules for Medium PRF Radar</b>		5a. CONTRACT NUMBER			
		5b. GRANT NUMBER			
		5c. PROGRAM ELEMENT NUMBER			
6. AUTHOR(S)		5d. PROJECT NUMBER			
		5e. TASK NUMBER			
		5f. WORK UNIT NUMBER			
7. PERFORMING ORGANIZATION NAME(S) AND ADDRESS(ES) <b>Department of Aerospace, Power and Sensors, Cranfield University, Royal Military College of Science, Shrivenham, Swindon, England,SN6 8LA.</b>		8. PERFORMING ORGANIZATION REPORT NUMBER			
9. SPONSORING/MONITORING AGENCY NAME(S) AND ADDRESS(ES)		10. SPONSOR/MONITOR'S ACRONYM(S)			
		11. SPONSOR/MONITOR'S REPORT NUMBER(S)			
12. DISTRIBUTION/AVAILABILITY STATEMENT <b>Approved for public release, distribution unlimited</b>					
13. SUPPLEMENTARY NOTES <b>See also ADM001798, Proceedings of the International Conference on Radar (RADAR 2003) Held in Adelaide, Australia on 3-5 September 2003. , The original document contains color images.</b>					
14. ABSTRACT					
15. SUBJECT TERMS					
16. SECURITY CLASSIFICATION OF:			17. LIMITATION OF ABSTRACT <b>UU</b>	18. NUMBER OF PAGES <b>6</b>	19a. NAME OF RESPONSIBLE PERSON
a. REPORT <b>unclassified</b>	b. ABSTRACT <b>unclassified</b>	c. THIS PAGE <b>unclassified</b>			

Multiple bursts of pulses are required in order to perform target detection and to resolve range and Doppler ambiguities. This is achieved by transmitting a number of PRFs within the dwell time on target and sequentially measuring and comparing the ambiguous information received from every PRF. All the eight PRFs from a 3 of 8 system must be able to be transmitted within the dwell time, with each PRF burst having 64 pulses (64-point FFT) and a short period of time in which to change over PRFs.

The positions of blind zones vary with PRF, therefore, by applying suitable PRFs in a multiple-PRF detection scheme, not only may range and Doppler ambiguities be resolved, but also the blind zones may be staggered to improve target visibility. Ground clutter returns received through the antenna sidelobes may be strong enough to overwhelm weak target signals, consequently blind ranges tend to worsen with increasing range.

In the blind zone map of Fig. 1, the black shading represents zones where fewer than  $M$  PRFs are clear and, hence, where the radar is totally blind. The grey shading represents the near-blind zones where exactly  $M$  PRFs are clear. White regions represent zones where  $(M+1)$  or more PRFs are clear.

The selection of PRFs in a medium PRF set is therefore based on the following:

- 1) A spread of values which enable the resolution of range and velocity ambiguities,
- 2) the minimisation of blind zones,
- 3) removal of totally blind velocities,
- 4) ensuring that the duty cycle yields the desired average transmitted power,
- 5) constraints imposed by the practical issues of system timings, e.g. transmitter duty cycle giving an upper bound on the allowable PRF, and average PRI being constrained by the target illumination time [4].

The finer the timing resolution of the PRIs, the greater the number of PRIs within the search space. This in turn increases the complexity of finding an optimum PRF set but also improves the performance of that optimum solution.

Since the minimisation of blind zones is influenced by the signal to clutter ratio, it is imperative to have a reliable model or data on the nature of the clutter. The exact clutter characteristics are likely to be scenario specific and so one must either operate using a PRF set appropriate to averaged conditions or optimise the PRF set dynamically. In section VI we consider the latter.

### III. BASIS OF 2 OF N DECODING

#### A. Decodability

Previous research into extending 3 of  $N$  methods [1], [2] have described autonomous methods for determining optimum 3 of  $N$  schedules. In general the decodability of  $M$  of  $N$  medium PRF waveforms requires (1) & (2) to be satisfied for all combinations of  $M$  PRFs in the set of  $N$ , where LCM is the lowest common multiple,  $R_{\max}$  is the maximum range

and  $D_{\max}$  is the maximum Doppler bandwidth.

$$\text{LCM}(\text{PRI}_1, \text{PRI}_2, \dots, \text{PRI}_M) \geq \frac{2R_{\max}}{c} \quad (1)$$

$$\text{LCM}(\text{PRF}_1, \text{PRF}_2, \dots, \text{PRF}_M) \geq D_{\max} \quad (2)$$

For airborne applications, low-PRF operation with  $M = 1$  will satisfy (1), but not (2). For high-PRF operation,  $M = 1$  will satisfy (2), but not (1). For limited ranges of range and Doppler, (1) & (2) can be satisfied with  $M = 1$ , for example in Battlefield Surveillance Radar. In the general case,  $M = 1$  does not satisfy both (1) & (2), therefore  $M > 1$  is required.

#### B. 2 of $N$ vs. 3 of $N$

The minimum number of PRFs in which target data is required in order to resolve range and velocity ambiguities is, strictly, two. 2 of  $N$  schedules require PRFs for which every combination of 2 from the  $N$  used satisfy (1) & (2). This is feasible if the PRI resolution is very fine since this results in a large number of PRIs / PRFs between the maximum and minimum limits and makes the decodability requirements of (1) & (2) easier to satisfy. Relatively coarse PRI resolution of one range cell, which is typical of many current systems, may prevent 2 of  $N$  schedules satisfying (1) & (2) and so data is required in a third PRF. This study assumes PRI resolution of 10ns and so 2 of  $N$  schedules are viable.

As  $M$  is increased, both the probability of detection and probability of false alarm reduce. As  $N$  increases, it becomes harder to transmit the  $N$  PRFs within the dwell time on the target. The more degrees of freedom are available ( $N - M$ ), the better the blindzone performance that can be achieved and the greater the number of targets that can be resolved unambiguously.

### IV. THE RADAR MODEL

A radar model based on an airborne fire control type application was derived to trial the fitness of PRF sets. The model assumes 10GHz operation, 64-point FFT processing, linear FM pulse compression achieving a compression ratio of 14 and that platform motion compensation is applied. The maximum target velocity with respect to the ground was taken as 1500 m/s and the maximum range was taken to be 185 km (100 nmi). These and other operational characteristics are summarised in Table I. It is intended that the model should be representative of the types currently in service or about to enter service. Clutter was modelled and resulted in a requirement to reject mainbeam clutter and ground moving targets over a band  $\pm 1.67\text{kHz}$ . Simulations were performed against a  $5\text{m}^2$  target and result in considerable blindness at long ranges due to overwhelming sidelobe clutter. Blindness is mapped for signal-to-clutter ratio less than 1. Larger targets are less easily swamped by sidelobe clutter and detection is maintained at greater ranges.

We envisage conventional range gating into  $0.5\mu\text{s}$  periods (=compressed pulse width) by virtue of ADC sampling periods of  $0.5\mu\text{s}$ . Since the PRIs are quantised in multiples of 10ns, the last sample period (range cell) is not likely to be coincident

TABLE I  
SUMMARY OF THE RADAR MODEL'S CHARACTERISTICS

Parameter	Value
Carrier frequency	10 GHz
Minimum PRI	35 $\mu$ s
Maximum PRI	150 $\mu$ s
Transmitted pulsewidth	7 $\mu$ s
Compressed pulsewidth	0.5 $\mu$ s
Compression technique	Linear FM 2 MHz chirp
FFT size	64 bins
Range resolution	75m
Blind range due to eclipsing	15 range cells
Duty cycle	Variable (0.2 peak)
Antenna 3dB beamwidth	3.9 °
Antenna scan rate	60 °/s
Maximum GMT velocity rejected	25 m/s
Mainlobe clutter/GMT rejection notch bandwidth	$\pm$ 1.67 kHz
Maximum target Doppler	$\pm$ 100 kHz (1500 m/s )
Maximum detection range	185.2 km (100 nmi)
Clutter backscatter coefficient	-20 dB
Target radar cross-section	5 m <sup>2</sup>

with the end of the receiving period, in the general case. Therefore, little target energy is likely to reside in the last range cell and the  $P_d$  in this cell will be degraded. During the transmitted pulse the ADC would be reset. Samples 1 to 14 coincide with the 7 $\mu$ s transmitted pulse and so are blanked. Sample 15 coincides with the transmit to receive changeover period and is also blanked. The receiver is finally opened by the beginning of the 16<sup>th</sup> sample period giving a total receiver blanking time of 7.5 $\mu$ s. The first range cell therefore coincides with ADC sample period 16. Echoes received within the first or last 13 range cells will be partially eclipsed due to the overlap of the uncompressed echo (duration of 7 $\mu$ s) with the receiver blanking period (= 7.5 $\mu$ s). Thus the SNR and hence the  $P_d$  will degrade over the last 13 range cells of the receiving period and will start low but gradually improve over the first 13 range cells. Nevertheless very large targets may be detectable within the last few range cells. Currently, blind ranges are calculated on the basis of blindness extending throughout samples 1 to 29 (the beginning of the transmitted pulse to 7.5 $\mu$ s after the end of the transmitted pulse). Various alternative protocols could be considered such as sharing the same blind range between the end of one receiving period and the start of the next. Whilst the optimisation process will yield different PRFs, their total blind zone performance is not likely to differ significantly from those found by the current scheme.

## V. EVOLUTIONARY ALGORITHMS AND THEIR APPLICATION TO THE PROBLEM

### A. Introduction

Evolutionary Algorithms are optimisation procedures which operate over a number of cycles (generations) and are designed

to mimic the natural selection process through evolution and survival of the fittest [5]. A *population* of potential PRF sets is maintained by the algorithm. Each potential PRF set is represented by one *chromosome*. This is the genetic description of the solution and may be broken into  $N$  sections called *genes*. Each gene represents a single PRF. The three simple operations found in nature; natural selection, mating and mutation are used to generate new chromosomes and therefore new potential solutions.

Each chromosome is evaluated at every generation using an *objective function* that is able to distinguish good solutions from bad ones and to score their performance. With each new generation, some of the old chromosomes are removed to make room for the new, improved offspring. Despite being very simple to code, requiring no directional or derivative information from the objective function and being capable of handling large numbers of parameters simultaneously, evolutionary algorithms can achieve excellent results.

The radar model accepts a chromosome from the evolutionary algorithm and decodes it into a set of PRIs. Operational parameters are passed to the clutter model, which in turn returns clutter data. A blind zone map is created and target visibility is determined. The raw visibility data is then passed back to the evolutionary algorithm as the objective value to drive the evolutionary process. A new generation of potential PRFs is then produced and the process repeated.

Each chromosome forms a trial solution to the problem and consists of a set of  $N$  genes that lie in the interval [0,1). These genes are then decoded into a PRI schedule, which is then used within a radar model to assess the schedule's quality and to ensure that the schedule meets certain constraints. For a 2 of N system, the chromosome is transformed into a PRI set by first generating a set,  $\mathcal{P}$ , containing all possible choices of PRI (11501 in the example in this paper). The first PRI is chosen as the  $i^{th}$  PRI with  $i$  given by the total number of available PRIs ( $|\mathcal{P}|$ ) multiplied by the value of the first gene, giving a choice of 1 in 11501. The PRI chosen is removed from the set  $\mathcal{P}$ . The remaining set  $\mathcal{P}$  is now checked and any PRIs that are not decodable in both range and Doppler with the first PRI chosen are removed from the set  $\mathcal{P}$ . Any PRIs that would also lead to a blind velocity are also pruned. The second and subsequent PRIs can now be chosen similarly, given the reduced set of  $\mathcal{P}$ , and reducing the set accordingly after choosing each PRI. This process will ensure that the PRI set is fully decodable. If  $|\mathcal{P}| = 0$  before all the PRIs are chosen, the objective is set to be totally blind.

The objective function provides a measure of how well an individual performs in the problem domain [5]. In this case, the objective function is the total area of the blind zone map (in metres Hertz) with  $M + 1$  or more PRFs clear. The decoding process has already ensured that the PRF set is fully decodable with reduced ghosting and no has blind velocities.

### B. Summary

The maximum transmitter duty cycle (20% ) constrains the maximum acceptable PRF to be 28.57kHz. The width of the

mainbeam clutter rejection notch ( $\pm 1.67\text{kHz}$ ) constrains the minimum PRF to be  $6.67\text{kHz}$ , allowing the clutter to occupy up to a maximum of half the PRF. The PRI constraints, combined with the chromosome transformation algorithm means all PRI sets are decodable, retain good target visibility and are not prone to blind velocities. Repeated generations of the evolutionary algorithm optimisation process continue to refine target visibility by minimising blind zones.

## VI. DYNAMIC SELECTION OF OPTIMAL PRF SETS

It has been demonstrated [1], [2] that an evolutionary algorithm can be used to identify optimal or near optimal PRI sets for the MPRF radar system. As the position and extent of the sidelobe clutter lines change with altitude, azimuth and elevation scan angle and anticipated target size, so must the PRF set to be transmitted in order to keep blind zones under control and to a minimum, possibly focusing the optimisation to reduce blind zones in specific regions to a minimum too.

As the platform conditions (for altitude and pitch etc.) change relatively slowly while the radar is in operation, the evolutionary algorithm can be used to select a new average PRF set every few seconds to account for changing altitude and velocity. With optimisation of the current code and the fact that decodable 2 of  $N$  schedules can be generated more quickly than 3 of  $N$  schedules, optimisation in real time is imminent.

On-line optimisation during each scan or even burst-to-burst (i.e. dwell-to-dwell) may be possible with future processing capabilities. Not only will dynamic optimisation provide the best performance in terms of blindzones, but will also improve resistance to detection by ESM systems and interruption or deception by countermeasures.

For optimum performance a good model of sidelobe clutter is required in order to establish the locations of the sidelobe clutter lines. It may be possible to use previous returns to estimate the true clutter distribution, and therefore use short-term measured data to form the clutter information for the different PRIs in the dynamic optimisation process.

## VII. COMPARISON OF 2 OF $N$ AND 3 OF $N$ SCHEDULES

### A. Blind Zone Performance

To assess the comparative performance of different PRI set schemes, representative trials have been performed using the radar model. One hundred trials of each method have been performed using an EA and near optimal PRI sets have been generated (for further details of the EA and radar model see [2]). Each trial used a population of 50 for 100 generations.

All blindness statistics are based on visibility in less than  $M+1$  PRFs and include blindness due to overwhelming sidelobe clutter and the first blind range (along the bottom of the map) and the first blind velocity (up the left hand side of the map). Table II summarises the results.

It is clear that 2 of 7 is better than 3 of 9. The 2 of 6 schedule is better than 3 of 8 but worse than 3 of 9. The 2 of 5 schedule is becoming quite blind. The constraint for blind velocity removal is particularly harsh in the 2 of 5 case

TABLE II

TABLE COMPARING BLINDZONE PERFORMANCE OF DIFFERENT  $M$  OF  $N$  SCHEMES (100 TRIALS EACH). FIGURES SHOW PERCENTAGE BLIND FOR EACH SCHEDULE

M of N	Min %	Max %	Mean %	Median %	$\sigma$ %
2 of 5	66.10	66.73	66.43	66.44	0.1434
3 of 8	58.37	59.91	59.01	59.02	0.2803
2 of 6	56.35	57.70	57.12	57.18	0.3316
3 of 9	53.74	55.02	54.46	54.51	0.2656
2 of 7	48.90	50.24	49.46	49.54	0.3437
2 of 8	44.13	45.21	44.59	44.57	0.2296

and restricts the performance of the 2 of 5 system severely. Decodability is simplest to achieve in a 2 of 5 system.

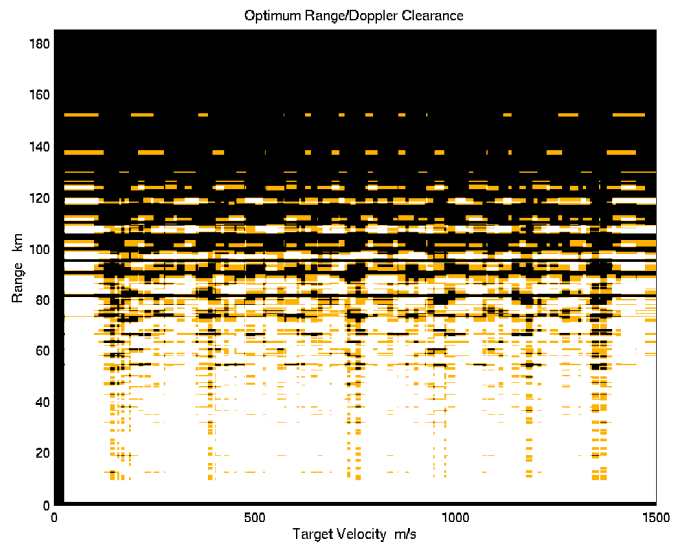


Fig. 1. Blind zone map for best 3 of 8 solution,  $5\text{ m}^2$  target

Figure 1 shows the blind zone map for the best 3 of 8 solution found. This solution represents the most common MPRF schedule. Table III shows the PRIs used, the mean PRI, mean duty cycle and range-Doppler area that is blind. For the radar model used and a 3 of 8 schedule, the mean PRI must be less than  $100.4\mu\text{s}$  (assuming  $65\text{ms}$  dwell time and  $1.7\text{ms}$  lost per PRI in change over). It is clear that the mean PRI of the optimised set is lower than the limit at  $88.77\mu\text{s}$ . The mean PRI identified could either be used with a scan rate of  $66.0^\circ/\text{s}$ , or dead time / built-in-test could be added at the end of the set of PRIs, as is used in many current radar systems. Often the scan rate is determined by subsequent processing but with phased array technology becoming more available in airborne systems, the pressure to allow a variable scan rate is increasing.

Figure 2 shows the blind zone map for the best 2 of 6 solution found. This solution gives fewer blind zones than the 3 of 8 solution, yet has two fewer PRIs. Table IV details the limits on mean PRI for different MPRF schedules. It is clear that the mean PRI could be much higher for a 2 of 6 schedule,

TABLE III  
PRI SET FOR BEST 3 OF 8 STRATEGY ( $\mu\text{s}$ )

	63.11	69.97	77.07	81.31	90.06	99.90	109.75	119.00
Mean PRI								88.77 $\mu\text{s}$
Mean duty cycle								7.89 %
Peak duty cycle								11.09 %
Min range/Doppler blindness (m.Hz)								1.0629 $e+10$

TABLE IV  
RANGE OF MEAN PRI LIMITS FOR DIFFERENT SCHEDULES

Schedule	Mean PRI
M of 6	142.7 $\mu\text{s}$
M of 7	118.5 $\mu\text{s}$
M of 8	100.4 $\mu\text{s}$
M of 9	86.3 $\mu\text{s}$

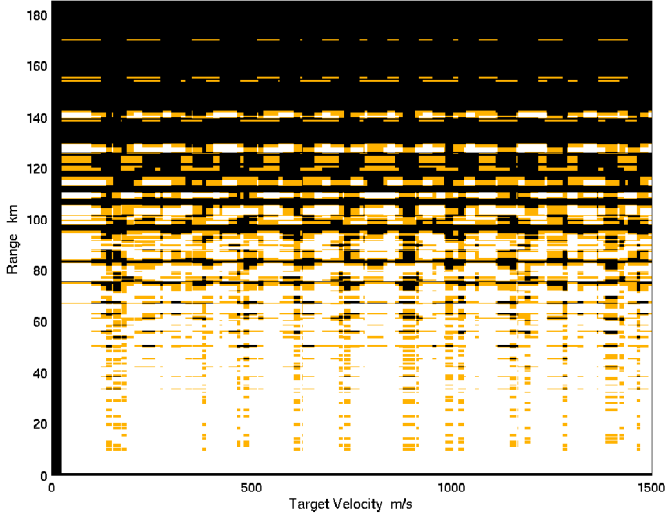


Fig. 2. Blind zone map for best 2 of 6 solution, 5  $m^2$  target

allowing a wider range of PRIs to be chosen. Table V shows the PRIs used, the mean PRI, mean duty cycle and range-Doppler area that is blind. By chance, the near-optimal set found has a relatively low mean PRI of 88.87 $\mu\text{s}$ , giving a total dwell time of 44.3ms, rather than the maximum 65ms. Most of this saving is because only six PRF changeover times need to be accommodated. The mean PRI identified could be used with a scan rate of 88.0 $^\circ/\text{s}$ .

Figure 3 shows the blind zone map for the best 2 of 7 solution found. This solution gives fewer blind zones than the 3 of 9 solution detailed in [2], yet again has two fewer PRIs. Again it is clear that the mean PRI could be higher for a 2 of 7 schedule, allowing a wider range of PRIs to be chosen. Table VI shows the PRIs used, the mean PRI, mean duty cycle and range-Doppler area that is blind. The mean PRI gives a total dwell time of 57.3ms, compared to the maximum 65ms. The mean PRI identified could be used with a scan rate of 68.0 $^\circ/\text{s}$ .

TABLE V  
PRI SET FOR BEST 2 OF 6 STRATEGY ( $\mu\text{s}$ )

	64.04	74.53	83.03	92.07	100.75	118.80
Mean PRI						88.87 $\mu\text{s}$
Mean duty cycle						7.88 %
Peak duty cycle						10.93 %
Min range/Doppler blindness (m.Hz)						1.0571 $e+10$

TABLE VI  
PRI SET FOR BEST 2 OF 7 STRATEGY ( $\mu\text{s}$ )

	73.55	81.03	89.76	99.42	109.50	116.46	140.17
Mean PRI							101.41 $\mu\text{s}$
Mean duty cycle							6.90 %
Peak duty cycle							9.52 %
Min range/Doppler blindness (m.Hz)							9.2137 $e+9$

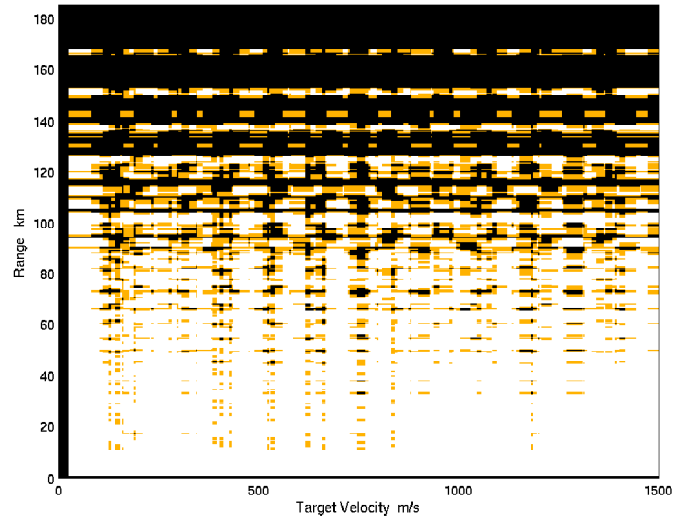


Fig. 3. Blind zone map for best 2 of 7 solution, 5  $m^2$  target

Figure 4 shows the blind zone map for the best 2 of 8 solution found. This solution gives far fewer blind zones than the 3 of 8 solution, yet again has the same number of PRIs. Table VII shows the PRIs used, the mean PRI, mean duty cycle and range-Doppler area that is blind. The mean PRI gives a total dwell time of 64.5ms and the mean PRI identified could be used with a scan rate of 60.49 $^\circ/\text{s}$ . It is clear that the optimisation has exploited the mean PRI limit to the full.

### B. Detection Performance

For a 2 of  $N$  system, the probability of detection is higher than 3 of  $N$  as only 2 PRIs require a detection. The function for probability of detection and false alarm for  $M$  of  $N$  and in the absence of targets is given in (3) & (4).

$$P_{d_{M \text{ of } N}} = \sum_{i=M}^N {}^N C_i P_d^i (1 - P_d)^{N-i} \quad (3)$$

TABLE VII  
PRI SET FOR BEST 2 OF 8 STRATEGY ( $\mu\text{s}$ )

	78.92	81.56	86.66	90.46	99.81	111.81	117.09	128.56
Mean PRI								99.36 $\mu\text{s}$
Mean duty cycle								7.05 %
Peak duty cycle								8.87 %
Min range/Doppler blindness (m.Hz)								8.3451e+9

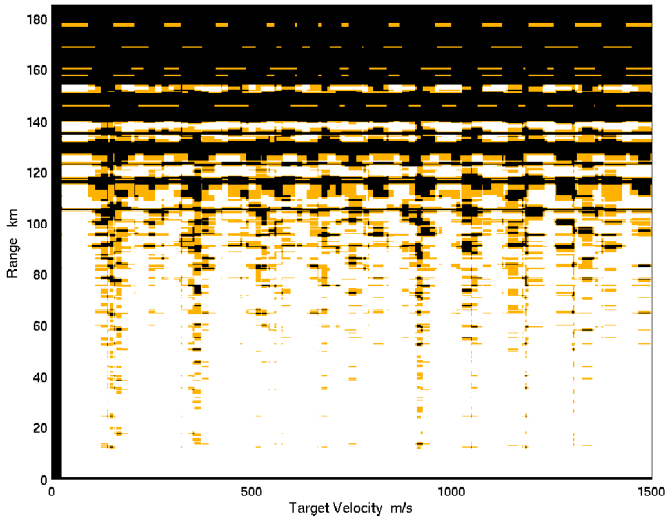


Fig. 4. Blind zone map for best 2 of 8 solution,  $5 \text{ m}^2$  target

$$P_{fa_{\text{MofN}}} = \sum_{i=M}^N {}^N C_i P_{fa}^i (1 - P_{fa})^{N-i} \quad (4)$$

Thus for a single  $P_d = 0.5$  and  $P_{fa} = 10^{-2}$ ,  $P_{d_{\text{MofN}}}$  for 2 of 7 is 0.94 compared to 0.86 for 3 of 8. Unfortunately, the overall probability of false alarm will increase as only two PRFs are being used for decoding. With the above example,  $P_{fa_{\text{MofN}}}$  for 2 of 7 is  $2.0 \times 10^{-3}$  compared to  $5.4 \times 10^{-5}$  for 3 of 8. To correct the final probability of false alarm to be equivalent to the 3 of 8 case, the detection threshold must be raised a little in order to achieve an input false alarm probability of  $P_{fa} = 1.6 \times 10^{-3}$ , a reduction of  $P_{fa}$  by a factor of 6. As probability of false alarm is very sensitive to the change of threshold, only a small change in threshold level would be required. This change would of course reduce the probability of detection a little, but in general the raising of the threshold will make the probability of detection and false alarm probabilities of the two approaches very similar. The 2 of 7 scheme though still has one less PRF. This allows longer PRIs to be used within the dwell, without upsetting the average PRI. This often allows a clearer blind zone map to be found than for a 3 of 8 system as the choice of PRI is less constrained.

It is acknowledged that the ghosting performance, in the presence of targets, of 2 of N schedules will be worse than that of 3 of N schedules and this is the subject of continued research.

## VIII. CONCLUSIONS

The evolutionary algorithm can select novel 2 of N near-optimal PRF sets efficiently, with modest computing effort and produce a significant improvement in radar detection performance. The ‘quality’ of each set is based on models of airborne fire control radar and associated clutter and so each PRF set is application/scenario specific.

Repeated runs of the evolutionary algorithm identify near-optimal PRF sets which differ marginally from each other. These repeats indicate the existence of several similar local optima in the problem space and the ability of the evolutionary algorithm to find them.

The evolutionary algorithm has optimised the selection of 2 of N schedules which may be transmitted within the target illumination time. The 2 of N schedules are simpler to transmit within the dwell time as overall fewer PRFs are required to achieve the same blind zone performance when compared to a 3 of N system. Typically, with a  $5 \text{ m}^2$  RCS target, 2 of 8 system and the particular clutter characteristics applied in the model, a 14% improvement in total range-Doppler blindness is achieved over a conventional 3 of 8 system, with the most noticeable improvement occurring at the medium and far detection ranges (60 to 150 Km), beyond which high sidelobe clutter levels are the dominant cause of blindness.

The evolutionary algorithm has also been developed to run quick enough to allow the optimisation of the selection to run dynamically in real time on a modern processing system.

## ACKNOWLEDGEMENTS

The authors would like to acknowledge the use of the Department of Aerospace, Power, and Sensors DEC Alpha Beowulf cluster for this research.

## REFERENCES

- [1] P. G. Davies and E. J. Hughes, “Medium PRF set selection using evolutionary algorithms,” *IEEE Transactions on Aerospace and Electronic Systems*, vol. 38, no. 3, pp. 933–939, July 2002.
- [2] Clive M. Alabaster, Evan J. Hughes, and John H. Matthew, “Medium PRF radar PRF selection using evolutionary algorithms,” *IEEE Transactions on Aerospace and Electronic Systems*, 2003, to Appear.
- [3] William H. Long and Keith A. Harringer, “Medium PRF for the AN/APG-66 radar,” *Proceedings of the IEEE*, vol. 73, no. 2, pp. 301–311, Feb. 1985.
- [4] R. A. Moorman and J. J. Westerkamp, “Maximizing noise-limited detection performance in medium PRF radars by optimizing PRF visibility,” in *Proceedings of the IEEE 1993 National Aerospace and Electronic Conference, NAECON 93*, 1993, vol. 1, pp. 288 – 293.
- [5] Kalyanmoy Deb, *Multi-objective optimization using evolutionary algorithms*, John Wiley & Sons, 2001, ISBN 0-471-87339-X.